



Evaluation of activity of Graves' orbitopathy with multiparameter orbital magnetic resonance imaging (MRI)

Jingyi Cheng^{1#}, Xiuying Zhang^{2#}, Jianxiu Lian³, Zhenyu Piao⁴, Lingli Zhou², Xinyi Gou¹, Chuhan Chen¹, Lei Chen¹, Ke Jiang³, Jin Cheng^{1^}, Linong Ji², Nan Hong¹

¹Department of Radiology, Peking University People's Hospital, Beijing, China; ²Department of Endocrinology, Peking University People's Hospital, Beijing, China; ³Philips Healthcare, Beijing, China; ⁴Department of Ophthalmology, Peking University People's Hospital, Beijing, China

Contributions: (I) Conception and design: X Zhang, J Cheng; (II) Administrative support: L Ji, N Hong; (III) Provision of study materials or patients: Z Piao, L Zhou; (IV) Collection and assembly of data: J Lian; X Gou, C Chen, K Jiang; (V) Data analysis and interpretation: JY Cheng, L Chen; (VI) Manuscript writing: All authors; (VII) Final approval of manuscript: All authors.

[#]These authors contributed equally to this work.

Correspondence to: Jin Cheng. Department of Radiology, Peking University People's Hospital, No. 11, Xizhimen South St., Beijing 100044, China. Email: chengjinkuph@outlook.com.

Background: When quantitative magnetic resonance imaging (MRI) is used to assess the activity of Graves' orbitopathy (GO), the examination is generally focused on a specific orbital tissue, especially the extraocular muscles (EOMs). However, GO usually involves the entire intraorbital soft tissue. The aim of this study was to use multiparameter MRI on multiple orbital tissues to distinguish the active and inactive GO.

Methods: From May 2021 to March 2022, consecutive patients with GO were prospectively enrolled at Peking University People's Hospital (Beijing, China) and divided into those with active disease and those with inactive disease based on a clinical activity score. Patients then underwent MRI, including sequences of conventional imaging, T1 mapping, T2 mapping, and mDIXON Quant. Width, T2 signal intensity ratio (SIR), T1 values, T2 values, and fat fraction of EOMs, as well as water fraction (WF) of orbital fat (OF), were measured. Parameters were compared between the 2 groups, and a combined diagnostic model was constructed using logistic regression analysis. Receiver operating characteristic analysis was used to test the diagnostic performance of the model.

Results: Sixty-eight patients with GO (27 with active GO, 41 with inactive GO) were included in the study. The active GO group had higher values of EOM thickness, T2 SIR, and T2 values, as well as higher WF of OF. The diagnostic model, which included EOM T2 value and WF of OF, demonstrated a good ability to distinguish between active and inactive GO (area under the curve, 0.878; 95% CI: 0.776–0.945; sensitivity, 88.89%; specificity, 75.61%).

Conclusions: A combined model incorporating the T2 value of EOMs and the WF of OF was able to identify cases of active GO, potentially offering an effective and noninvasive method to assess pathological changes in this disease.

Keywords: Multiparameter magnetic resonance imaging evaluation (multiparameter MRI evaluation); quantitative magnetic resonance technology (quantitative MR technology); Graves' orbitopathy; fat fraction; water fraction

Submitted Aug 02, 2022. Accepted for publication Dec 21, 2022. Published online Feb 06, 2023.

doi: 10.21037/qims-22-814

View this article at: <https://dx.doi.org/10.21037/qims-22-814>

[^] ORCID: 0000-0002-1199-1351.

Introduction

Graves' orbitopathy (GO) is an inflammatory autoimmune disease. The remodeling of the orbit that occurs with this disease can lead to a number of complications, including photophobia, proptosis, eyelid retraction, and even vision loss (1). GO is considered a biphasic disease (2). In the active stage of the disease, an inflammatory reaction is prominent, making the condition potentially responsive to immunosuppressive therapy. However, the inactive stage of the disease mainly manifests as fibrosis and fat deposition (3).

The activity of GO is usually assessed using a clinical activity score (CAS) (4,5), which is recommended by the European Group on Graves' Orbitopathy (EUGOGO) guideline (6), but it is mainly based on clinical symptoms and is highly subjective (7). An accurate CAS assessment requires the assessor to have extensive experience in this specific field and access to specialist instruments, which may be difficult to obtain in most hospitals (8). Furthermore, the active phase of GO may be difficult to distinguish from the inactive phase based on CAS criteria (9). The ability to accurately and objectively distinguish between the active and inactive GO is crucial to treatment decision-making for patients with this condition (4).

Because magnetic resonance imaging (MRI) can provide high-resolution soft tissue imaging, this modality is widely used for the clinical diagnosis of GO. More specifically, quantitative magnetic resonance (MR) technology such as T1 mapping, T2 mapping, and mDIXON Quant sequences can provide the information needed to differentiate among various pathological processes. T1 value is the spin-lattice or longitudinal relaxation time of tissue; this value is used to assess the deposition of fibrous tissue (10,11). T2 value is defined as the spin-spin or transverse relaxation and is a time constant of transverse magnetization decay, which reflects extraocular muscle (EOM) edema and inflammation (12). In addition, fat fraction (FF) and water fraction (WF) can be calculated by separating fat and water signals on mDIXON Quant sequences (13). Research has shown that decreased T1 values and elevated FFs are associated with fat infiltration in EOMs, which is one characteristic of chronic and inactive phase GO (14-16).

Previous imaging studies have mainly focused on this association between inactive GO and fat infiltration in EOMs. However, several studies have assessed orbital fat (OF) tissues or lacrimal glands individually (17,18). These studies were limited, however, in that GO may involve all periocular and retrobulbar tissues, including lacrimal

glands, conjunctiva, EOMs, and OF, thus leading to complex changes in T1 values, T2 values, and FFs.

In this study, we hypothesize that multiparameter MRI-based diagnosis of GO activity would be more accurate when considering the combined model with more information of pathology and imaging. We present the following article in accordance with the STARD reporting checklist (available at <https://qims.amegroups.com/article/view/10.21037/qims-22-814/rc>).

Methods

Patients

This observational prospective study was approved by the Ethics Review Committee of Peking University People's Hospital (No. 2022PHB123-001). Since this was a purely observational study based on routine imaging examination, individual consent was waived by the Ethics Review Committee. The study was in compliance with the Health Insurance Portability and Accountability Act (HIPAA) and the Declaration of Helsinki (as revised in 2013).

From May 2021 to March 2022, consecutive patients diagnosed with GO at Peking University People's Hospital, Beijing, China were considered for study inclusion based on the following inclusion criteria: (I) pretreatment orbital MRI was performed; (II) interval between GO diagnosis and MRI examination was <1 week. (III) MR image quality was adequate for further analysis. Exclusion criteria were as follows: (I) disease duration was >18 months; (II) thyroid function was uncontrolled; (III) history of glucocorticoid therapy, radiotherapy, or surgical decompression; (IV) patient's vision was threatened. GO was diagnosed based on Bartley's diagnostic criteria (19). Two senior physicians who were blinded to the MRI results (an endocrinologist and an ophthalmologist both with >10 years of experience) determined the 7-point CAS and severity for each eye independently according to the EUGOGO atlas and guidelines (6). The CAS included assessment of spontaneous retrobulbar pain, pain on attempted upward or downward gaze, redness of eyelids, redness of conjunctiva, swelling of caruncle or plica, swelling of eyelids, and swelling of conjunctiva (chemosis) (20). In cases of disagreement, consensus was reached between the 2 physicians via discussion of the CAS and severity. CAS ≥ 3 for either eye was considered to indicate the presence of active GO. For each patient, the eye with the higher CAS was used for the analysis. Disease severity was classified as mild, moderate

Table 1 Detailed scan parameters for all sequences used

Parameters	Repetition time/echo time (ms)	Field of view (mm ³)	Voxel (mm ²)	Slice thickness/gap (mm)	Plane
T2-weighted imaging	2,500/80	200×200	0.6×0.75	2.5/0.25	Axial/coronal
T2-weighted imaging	3,000/80	150×150	0.6×0.75	2.5/0.25	Sagittal
T1-weighted imaging	519/20	200×200	0.65×0.85	2.5/0.25	Axial
T1 mapping	2/1	200×200	2×2	2.5/0	Coronal
T2 mapping	1,017/n*9	200×200	2×2	2.5/0	Coronal
mDIXON Quant	6.3/1.07	200×200	2.07×2.07	2.5/–1.25	Coronal

to severe, or sight-threatening based on the EUGOGO guidelines.

Demographic data, including patient sex, age, and disease duration, were collected at the first clinical visit. Disease duration was defined as the interval between the onset of GO-associated clinical symptoms and the date of the MRI examination. Information about history of Grave's disease (GD) (including duration and treatment) and smoking was also recorded. Thyroid function was assessed by monitoring serum thyroid-stimulating hormone, free triiodothyronine, and free thyroxine levels. Thyrotropin receptor antibody concentrations were also recorded.

MRI acquisition and processing

MRI examinations were performed on a 3.0 T system (Ingenia, Philips Healthcare, the Netherlands) with a 16-channel head coil. Patients were required to lie in a supine position with their eyes closed naturally. They were also instructed to look forward and to keep their eyes still. The scanning parameters of the MR sequences used are shown in *Table 1*.

Conventional structural imaging included axial T1-weighted imaging; axial T2-weighted imaging; and axial, coronal, and oblique sagittal T2-weighted imaging with fat-suppression sequences. The axial scanning line was parallel to the auditory canthus, and the oblique sagittal line was parallel to the optic nerve. In the cross-sectional T2 weighted images, the largest slice of the internal and external oblique muscle belly was selected to locate the coronal scanning slices of T1 mapping, T2 mapping, and mDIXON Quant sequences.

Image analysis

MRI data were evaluated separately by 2 senior radiologists

(with >10 years of experience) who were blinded to the clinical information, including CAS. Image data from coronal T1 mapping, coronal T2 mapping, mDIXON Quant, and coronal T2-weighted imaging with fat suppression were assessed using a postprocessing software platform (IntelliSpace Portal, Philips Healthcare, the Netherlands). On the T1 mapping, T2 mapping, and mDIXON Quant images, a circular region of interest (ROI) was manually drawn along the borderlines of the medial, external, superior, and inferior rectus muscles of both eyes. The mean values of T1, T2, and FF for the 8 EOMs of each patient were measured and recorded (*Figure 1*). Another ROI (about 10–15mm²) was manually drawn in the lateral upper quadrant OF on mDIXON Quant images of water and fat, and the average signal intensity (SI) in the ROIs was measured. For the assessment of OF edema, the WF of OF was calculated as $SI_{\text{water}} / (SI_{\text{water}} + SI_{\text{fat}})$ (18) (*Figure 1*). For coronal T2-weighted imaging with fat-suppression sequences, 8 ROIs were placed as above, the mean value of the measured SI was taken as SI_{EOM} . An ROI (about 10–15 mm²) was then placed in the temporal muscle, and the mean SI of the ROI was recorded as $SI_{\text{temporal muscle}}$. The SI ratio (SIR) was defined as $SI_{\text{EOM}} / SI_{\text{temporal muscle}}$ (14) (*Figure 1*).

The maximum width or thickness of the EOMs was measured on T2-weighted fat-suppression sequences. Because the muscle belly of the superior rectus muscle and the levator palpebrae muscle were relatively close and difficult to distinguish, they were combined in measurements as the “superior complex”. The maximum thickness of the superior complex and inferior rectus muscle was measured on oblique sagittal images, and the maximum width of the internal and external rectus muscle was measured on axial images. The measurements of width/thickness for 8 EOMs in each patient were then averaged and recorded (*Figure 2*).

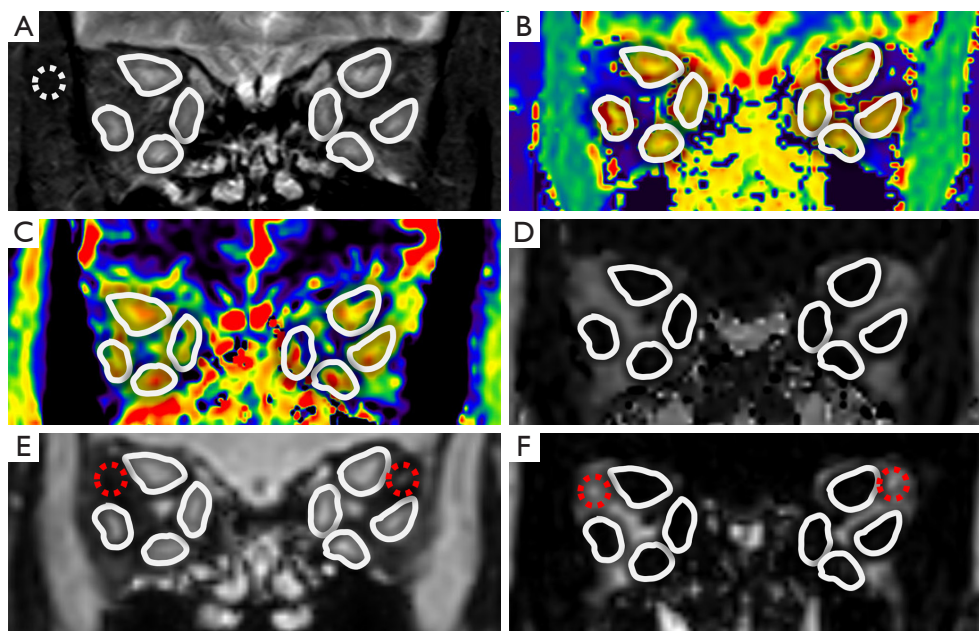


Figure 1 Images (coronal plane) from a 60-year-old woman with Graves' orbitopathy. ROIs were placement of 8 extraocular muscles on T2-weighted image with fat suppression (A), T1 mapping (B), T2 mapping (C) and mDIXON Quant sequences, including fat fraction (D), and water (E) and fat (F) phases are shown (white solid circles). ROIs of WF of orbital fat (E,F) (red dotted circles) and temporal muscle (A) (white dotted circle) were shown. ROIs, regions of interest; WF, water fraction.



Figure 2 Quantitative measurements of the width/thickness of 8 extraocular muscles on axial (A) and coronal (B) T2-weighted images with fat suppression.

Statistical analysis

Categorical variables were described as number (n) and percentage (%). Quantitative variables were reported as mean \pm standard deviation (mean \pm SD) or median and interquartile range [median (Q1, Q3)] based on normal distribution analysis. To test the reproducibility of the quantitative parameters, we calculated the interclass correlation coefficients (ICCs). Differences in clinical and imaging characteristics between patients with active

GO and those with inactive GO were compared using independent sample *t*-tests, Mann-Whitney U tests, χ^2 tests, or Fisher exact tests. Binary logistic regression was used to select parameters and construct a combined model to identify active GO. Receiver operating characteristic (ROC) curves were calculated to assess sensitivity and specificity, and the areas under the ROC curve (AUC) values for the above parameters were also calculated to evaluate diagnostic efficacy. DeLong's test was used to evaluate the diagnostic performance of different methods. All data were analyzed

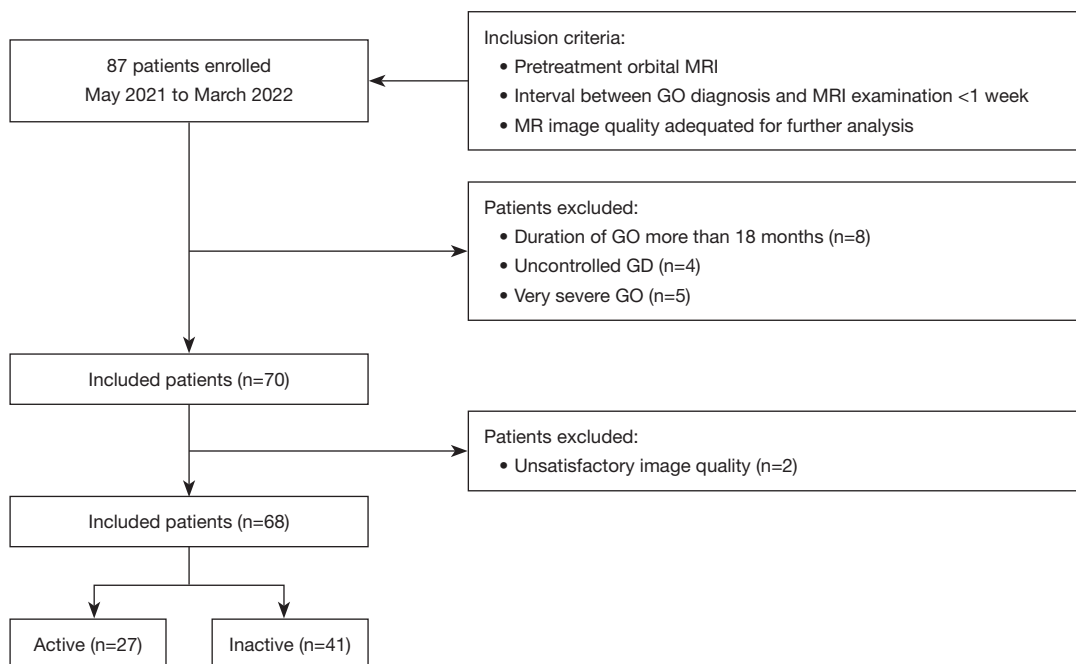


Figure 3 Flow chart of patient enrollment. MRI, magnetic resonance imaging; MR, magnetic resonance; GO, Graves' orbitopathy; GD, Grave's disease.

using IBM SPSS statistical version 25.0 and MedCalc version 20. A P value <0.05 was considered statistically significant.

Results

Demographics and clinical characteristics

A flow chart of patient enrollment is shown in *Figure 3*. A total of 68 patients (25 men, 43 women; age, 43.5 ± 13.1 years; range, 20–83 years) were enrolled in this study. Of these study patients, 27 (10 men, 17 women; age, 48.8 ± 12.4 years) had active GO and 41 (15 men, 26 women; age, 40.7 ± 12.8 years) had inactive GO. The mean CAS values were 3.22 ± 0.58 in the active group and 1.24 ± 0.80 in the inactive group. Ten of the 68 patients (14.7%) had different CAS scores for each eye; of these patients, no patient had disease classified differently in each eye (active/inactive GO). Patients with GD had been treated with methimazole (n=50), surgical resection (n=3), or ^{131}I therapy (n=3). The remaining 12 patients had no history of GD. There were no significant differences between the active and inactive groups in terms of laboratory test results, severity of GO, duration of GO/GD, and treatment history (*Table 2*).

Comparison of MR quantitative measurements

The ICC values between the 2 radiologists were good or excellent for each parameter and for all patients. The thickness, SIR, T2 values, and FF of EOMs were significantly higher in patients with active GO than in those with inactive GO (*Table 3*). However, there was no significant difference between the groups in T1 values.

Utility of MRI parameters to identify active GO

Forward stepwise logistic regression analysis was performed, using the T2 values of EOMs (P=0.02) and the WF of OF (P=0.05) as independent factors to distinguish between active and inactive GO. These 2 parameters were then used in the combined model to identify active GO. Activity and MRI diagnosis were shown in *Table 4*. The combined model demonstrated a favorable diagnostic performance in identifying active GO (AUC =0.878, 95% CI: 0.776–0.945), with a sensitivity of 88.89% and a specificity of 75.61% (*Table 4; Figure 4*). There were significant differences in AUCs between the combined model and models separately assessing the T2 values of EOMs (P=0.02) or the WF of OF (P=0.03).

Table 2 Patient demographics for active and inactive GO groups

Variables	Active GO (n=27)	Inactive GO (n=41)	P value
Age (year)*	48.8±12.4	40.7±12.8	0.01
Sex (M/F)*	10 (37.0)/17 (63.0)	15 (36.6)/26 (63.4)	0.05
Active smoker (y/n)*	1 (3.7)/26 (96.3)	3 (7.3)/38 (92.7)	1.00
Duration of GO (month)*	13.30±13.80	9.94±10.70	0.38
Duration of GD (month)*	16.62±31.20	17.57±28.10	0.90
Treatment for GD (y/n)*	20 (74.1)/7 (25.9)	36 (87.8)/5 (12.2)	0.17
Severity of GO (mild/moderate to severe)*	15 (55.6)/12 (44.4)	28 (68.3)/13 (31.7)	0.29
Proptosis (y/n)*	12 (44.4)/15 (55.6)	21 (51.2)/20 (48.8)	0.59
Eyelid retraction (y/n)*	10 (37.0)/17 (63.0)	7 (17.1)/34 (82.9)	0.07
Diplopia (y/n)*	7 (26.0)/20 (74.0)	6 (14.6)/35 (85.4)	0.25
Duction (y/n)*	10 (37.0)/17 (63.0)	8 (19.5)/33 (80.5)	0.11
Thyroid-stimulating hormone level (μIU/mL) [†]	1.49 (0.05, 4.47)	1.03 (0.03, 2.48)	0.38
Free triiodothyronine level (pmol/L) [†]	4.92 (4.44, 6.00)	4.94 (4.57, 5.33)	0.89
Free thyroxine level (pmol/L) [†]	16.54 (13.53, 18.00)	16.67 (14.02, 19.06)	0.57
Thyrotropin receptor antibody concentration (IU/L) [†]	5.47 (2.70, 12.35)	6.12 (2.48, 13.30)	0.81

*, mean ± standard deviation; **, n (%); †, median (interquartile range). GO, Graves' orbitopathy; y, yes; n, no; GD, Graves' disease.

Table 3 MRI parameters in active and inactive GO groups

Parameters	Active GO*	Inactive GO*	P value
Thickness of EOMs (mm)	5.46±1.28	4.60±1.15	0.02
T2 SIR of EOMs	2.64±0.45	2.17±0.60	0.004
T1 value of EOMs (ms)	1,514.30±158.91	1,439.70±126.15	0.06
T2 value of EOMs (ms)	88.73±9.30	77.78±6.98	<0.001
FF of EOMs	0.09±0.05	0.13±0.05	0.01
WF of OF	0.24±0.09	0.17±0.04	<0.001

*, mean ± standard deviation. MRI, magnetic resonance imaging; GO, Graves' orbitopathy; EOMs, extraocular muscles; SIR, signal intensity ratio; FF, fat fraction; WF, water fraction; OF, orbital fat.

Discussion

In this study, we found that a combined model including the T2 values of EOMs and the WF of OF had favorable accuracy in identifying active GO. The diagnostic performance of this combined model was better than the performance of either single-parameter model. Furthermore, significant differences were observed between active and inactive GO in terms of EOM thickness, SIR, and FF.

To our knowledge, this is the first study to offer a combined model for identifying active GO in which MRI quantitative parameters for multiple tissues (EOM and OF) and multiple MRI sequences (T2 mapping and mDIXON Quant) were included. As GO is a complex condition involving nearly all of the tissues of the orbit, a combined model may offer a more comprehensive assessment than methods focusing on single orbital tissues, such as the CAS score, which is mainly limited to the evaluation of symptoms in the anterior part of orbit. It can provide objective and

Table 4 Diagnostic performance for T2 value of EOMs, WF of OF, and a combined model in distinguishing between active and inactive GO

Category	T2 value of EOMs				WF of OF				T2 value + WF			
	Wrong	Right	χ^2	P value	Wrong	Right	χ^2	P value	Wrong	Right	χ^2	P value
CAS, n	14	54	23.119	<0.001	35	33	8.552	0.003	34	34	27.087	<0.001
Active	13	14			8	19			3	24		
Inactive	1	40			27	14			31	10		
AUC (95% CI)	0.745 (0.625–0.843)				0.760 (0.644–0.858)				0.878 (0.776–0.945)			
Sensitivity (95% CI) (%)	48.15 (28.70–68.10)				70.37 (49.80–86.20)				88.89 (70.80–97.6)			
Specificity (95% CI) (%)	97.56 (87.10–99.90)				73.17 (57.10–85.80)				75.61 (59.70–87.60)			

CAS, clinical activity score; EOMs, extraocular muscles; WF, water fraction; OF, orbital fat; GO, Graves' orbitopathy; AUC, area under the curve; CI, confidence interval.

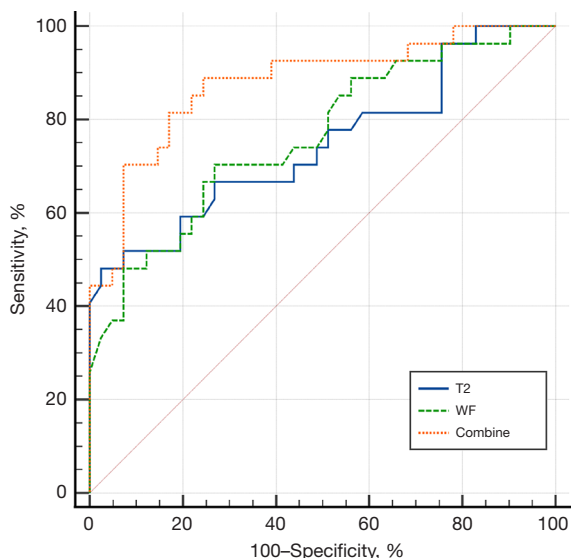


Figure 4 ROC analysis results for each MRI parameter and for the combined model in identifying cases of active Graves' orbitopathy. MRI, magnetic resonance imaging; ROC, receiver operating characteristic; WF, water fraction.

quantitative basis for the subjective CAS score, so as to be more confident in the formulation of treatment strategies. Then it could potentially provide biomarkers indicating the need for immunosuppressive treatment in patients with GO. Furthermore, MR-based quantitative indicators can be compared before and after treatment, which is the basis for curative effect.

The pathological characteristics of active GO mainly involve inflammatory edema caused by glycosaminoglycan deposition between EOM fibers and lymphocyte infiltration (21). However, inactive GO generally involves

either orbital fibrosis and fat infiltration, which occur in the chronic phase of the disease (2), or mild edema, which occurs in the early stages of the disease. These manifestations of inactive GO generally occur in the absence of inflammatory edema. Because an increase in water content may be reflected by an increase in T2 values (15), the value of T2 in patients with active GO is expected to be higher than in patients with inactive GO, which was confirmed in our study. A previous study demonstrated that T2 values could be used to differentiate between patients with GO and healthy controls and that these values could also be used to evaluate the response to immunosuppressive treatment (15). These and other previous findings suggest that T2 mapping may be useful in the evaluation of GO activity and in the assessment of the inflammatory state of EOMs (15,22).

Redundant glycosaminoglycan may also be deposited in other orbital tissues during the active phase of GO. In a previous study, the T2-weighted imaging SIR of OF was significantly positively correlated with CAS, indicating that OF inflammation may reflect GO activity (17). Because the T2 value of normal fat is obviously higher than that of muscle, the high T2 signal in orbital would be contributed more by fat than water (15). Then increased water content in OF may not be reflected by an increase in T2 values. In this study, the mDIXON Quant sequence was used to provide separation of water and fat on the same image, thus allowing us to observe a significant difference between active and inactive GO in the WF of OF. This finding, which reflected the inflammatory edema present in the OF, is similar to results from a previous study (18). The WF of OF was therefore selected as one of the parameters included in the combined model for identifying active GO.

EOM thickening is a common ocular manifestation of GO. In Bynu's research, volumes of several intraorbital structures, including EOM thickening could differentiate active GOs from inactive GOs (23). However, there were controversial results to use this parameter to distinguish inflammatory activity in GO, as this thickening may also be seen in patients with inactive GO (24). In our study, we also found that the thickness of EOMs in active GO was significantly higher than in inactive GO. This may have occurred because the thickening of EOMs was uneven in study patients, and we used the maximum value to expansion the differences. In addition, most study patients had only a short disease. Thus, the clinical manifestation of patients with inactive GO were close to normal EOMs, which is different with patients with chronic disease, representing EOMs with fibrotic enlargement (25). Nevertheless, thickening of EOMs has not been selected as the diagnosing parameter, while T2 value compensated for its diagnostic limitations with more sensitivity to present edema.

Some previous studies have used T1 mapping to distinguish between active and inactive GO (14,16), based on the principle that fat infiltration of the EOMs is predominant in the chronic phase and that the T1 values of fat are lower than those of normal muscle tissue. In our study, we observed no significant difference in T1 values between cohorts. However, most patients in our study had disease of short duration, suggesting that they were still in the early stages of GO and that fat infiltration of the EOMs had not yet occurred (2).

This study had several limitations. First, the sample size of this study was relatively small, and all patients were from single institution. then the generalizability of this diagnosing method should be testified in the future. Second, this was a cross-sectional study, then additional follow-up is needed to confirm the validity of these results. Third, there were significant differences between the active and inactive GO cohorts in age. However, previous research has found that demographic characteristics do not affect the disease course of GO (8).

In conclusion, this study demonstrated that active phase GO is associated with higher values of EOM thickness, SIR, and T2 and with higher values of WF of OF. Furthermore, the T2 value of EOMs and the WF of OF, when included in a combined diagnostic model, were able to distinguish between active and inactive GO in patients with disease of short duration.

Acknowledgments

We thank Mrs. Megan Griffith (megangriffith97@gmail.com) for English editing for this article.

Funding: None.

Footnote

Reporting Checklist: The authors have completed the STARD reporting checklist. Available at <https://qims.amegroups.com/article/view/10.21037/qims-22-814/rc>

Conflicts of Interest: All authors have completed the ICMJE uniform disclosure form (available at <https://qims.amegroups.com/article/view/10.21037/qims-22-814/coif>). Jianxiu Lian and Ke Jiang are employees of Philips Healthcare. The other authors have no conflicts of interest to declare.

Ethical Statement: The authors are accountable for all aspects of the work in ensuring that questions related to the accuracy or integrity of any part of the work are appropriately investigated and resolved. The study was approved by the Ethics Review Committee of Peking University People's Hospital (No. 2022PHB123-001). Since this was a purely observational study based on routine imaging examination, individual consent was waived by the Ethics Review Committee. The study was in compliance with the Health Insurance Portability and Accountability Act (HIPAA) and the Declaration of Helsinki (as revised in 2013).

Open Access Statement: This is an Open Access article distributed in accordance with the Creative Commons Attribution-NonCommercial-NoDerivs 4.0 International License (CC BY-NC-ND 4.0), which permits the non-commercial replication and distribution of the article with the strict proviso that no changes or edits are made and the original work is properly cited (including links to both the formal publication through the relevant DOI and the license). See: <https://creativecommons.org/licenses/by-nc-nd/4.0/>.

References

1. Kamboj A, Lause M, Kumar P. Ophthalmic manifestations of endocrine disorders-endocrinology and the eye. *Transl*

- Pediatr* 2017;6:286-99.
2. Dolman PJ. Grading Severity and Activity in Thyroid Eye Disease. *Ophthalmic Plast Reconstr Surg* 2018;34:S34-40.
 3. Heufelder AE. Pathogenesis of ophthalmopathy in autoimmune thyroid disease. *Rev Endocr Metab Disord* 2000;1:87-95.
 4. Bartalena L, Baldeschi L, Boboridis K, Eckstein A, Kahaly GJ, Marcocci C, Perros P, Salvi M, Wiersinga WM; European Group on Graves' Orbitopathy (EUGOGO). The 2016 European Thyroid Association/European Group on Graves' Orbitopathy Guidelines for the Management of Graves' Orbitopathy. *Eur Thyroid J* 2016;5:9-26.
 5. Mourits MP, Prummel MF, Wiersinga WM, Koornneef L. Clinical activity score as a guide in the management of patients with Graves' ophthalmopathy. *Clin Endocrinol (Oxf)* 1997;47:9-14.
 6. Smith TJ. Comment on the 2021 EUGOGO Clinical Practice Guidelines for the Medical Management of Graves' Orbitopathy. *Eur J Endocrinol* 2021;185:L13-4.
 7. Mawn LA, Dolman PJ, Kazim M, Strianese D, Genol I, Chong KKL, Sullivan TJ, Korn BS, Naik M, Dutton J, Velasco E Cruz A, Li C. Soft Tissue Metrics in Thyroid Eye Disease: An International Thyroid Eye Disease Society Reliability Study. *Ophthalmic Plast Reconstr Surg* 2018;34:544-6.
 8. Wu D, Zhu H, Hong S, Li B, Zou M, Ma X, Zhao X, Wan P, Yang Z, Li Y, Xiao H. Utility of multi-parametric quantitative magnetic resonance imaging of the lacrimal gland for diagnosing and staging Graves' ophthalmopathy. *Eur J Radiol* 2021;141:109815.
 9. Dickinson AJ, Perros P. Controversies in the clinical evaluation of active thyroid-associated orbitopathy: use of a detailed protocol with comparative photographs for objective assessment. *Clin Endocrinol (Oxf)* 2001;55:283-303.
 10. Tachibana S, Murakami T, Noguchi H, Noguchi Y, Nakashima A, Ohyabu Y, Noguchi S. Orbital magnetic resonance imaging combined with clinical activity score can improve the sensitivity of detection of disease activity and prediction of response to immunosuppressive therapy for Graves' ophthalmopathy. *Endocr J* 2010;57:853-61.
 11. Taylor AJ, Salerno M, Dharmakumar R, Jerosch-Herold M. T1 Mapping: Basic Techniques and Clinical Applications. *JACC Cardiovasc Imaging* 2016;9:67-81.
 12. Messrogli DR, Moon JC, Ferreira VM, Grosse-Wortmann L, He T, Kellman P, Mascherbauer J, Nezafat R, Salerno M, Schelbert EB, Taylor AJ, Thompson R, Ugander M, van Heeswijk RB, Friedrich MG. Clinical recommendations for cardiovascular magnetic resonance mapping of T1, T2, T2* and extracellular volume: A consensus statement by the Society for Cardiovascular Magnetic Resonance (SCMR) endorsed by the European Association for Cardiovascular Imaging (EACVI). *J Cardiovasc Magn Reson* 2017;19:75.
 13. Serai SD, Dillman JR, Trout AT. Proton Density Fat Fraction Measurements at 1.5- and 3-T Hepatic MR Imaging: Same-Day Agreement among Readers and across Two Imager Manufacturers. *Radiology* 2017;284:244-54.
 14. Chen L, Chen W, Chen HH, Wu Q, Xu XQ, Hu H, Wu FY. Radiological Staging of Thyroid-Associated Ophthalmopathy: Comparison of T1 Mapping with Conventional MRI. *Int J Endocrinol* 2020;2020:2575710.
 15. Das T, Roos JCP, Patterson AJ, Graves MJ, Murthy R. T2-relaxation mapping and fat fraction assessment to objectively quantify clinical activity in thyroid eye disease: an initial feasibility study. *Eye (Lond)* 2019;33:235-43.
 16. Matsuzawa K, Izawa S, Kato A, Fukaya K, Matsumoto K, Okura T, Miyazaki D, Kurosaki M, Fujii S, Taniguchi SI, Kato M, Yamamoto K. Low signal intensities of MRI T1 mapping predict refractory diplopia in Graves' ophthalmopathy. *Clin Endocrinol (Oxf)* 2020;92:536-44.
 17. Higashiyama T, Iwasa M, Ohji M. Quantitative Analysis of Inflammation in Orbital Fat of Thyroid-associated Ophthalmopathy Using MRI Signal Intensity. *Sci Rep* 2017;7:16874.
 18. Kaichi Y, Tanitame K, Terada H, Itakura H, Ohno H, Yoneda M, Takahashi Y, Akiyama Y, Awai K. Thyroid-associated Orbitopathy: Quantitative Evaluation of the Orbital Fat Volume and Edema Using IDEAL-FSE. *Eur J Radiol Open* 2019;6:182-6.
 19. Bartley GB, Gorman CA. Diagnostic criteria for Graves' ophthalmopathy. *Am J Ophthalmol* 1995;119:792-5.
 20. Wiersinga WM, Perros P, Kahaly GJ, Mourits MP, Baldeschi L, et al. Clinical assessment of patients with Graves' orbitopathy: the European Group on Graves' Orbitopathy recommendations to generalists, specialists and clinical researchers. *Eur J Endocrinol* 2006;155:387-9.
 21. Taylor PN, Zhang L, Lee RWJ, Muller I, Ezra DG, Dayan CM, Kahaly GJ, Ludgate M. New insights into the pathogenesis and nonsurgical management of Graves orbitopathy. *Nat Rev Endocrinol* 2020;16:104-16.
 22. Hou K, Ai T, Hu WK, Luo B, Wu YP, Liu R. Three dimensional orbital magnetic resonance T2-mapping in the evaluation of patients with Graves' ophthalmopathy. *J Huazhong Univ Sci Technolog Med Sci* 2017;37:938-42.
 23. Byun JS, Moon NJ, Lee JK. Quantitative analysis of orbital

- soft tissues on computed tomography to assess the activity of thyroid-associated orbitopathy. *Graefes Arch Clin Exp Ophthalmol* 2017;255:413-20.
24. Politi LS, Godi C, Cammarata G, Ambrosi A, Iadanza A, Lanzi R, Falini A, Bianchi Marzoli S. Magnetic resonance imaging with diffusion-weighted imaging in the evaluation of thyroid-associated orbitopathy: getting below the tip of the iceberg. *Eur Radiol* 2014;24:1118-26.
25. Lee JY, Bae K, Park KA, Lyu IJ, Oh SY. Correlation between Extraocular Muscle Size Measured by Computed Tomography and the Vertical Angle of Deviation in Thyroid Eye Disease. *PLoS One* 2016;11:e0148167.

Cite this article as: Cheng J, Zhang X, Lian J, Piao Z, Zhou L, Gou X, Chen C, Chen L, Jiang K, Cheng J, Ji L, Hong N. Evaluation of activity of Graves' orbitopathy with multiparameter orbital magnetic resonance imaging (MRI). *Quant Imaging Med Surg* 2023;13(5):3040-3049. doi: 10.21037/qims-22-814